Construction and Building Materials 147 (2017) 352–361

Contents lists available at ScienceDirect

Construction and Building Materials

journal homepage: www.elsevier.com/locate/conbuildmat

Influence of internal relative humidity and mix design of radiation shielding concrete on air permeability index

Wojciech Kubissa [a,*], Michał A. Glinicki [b]

[a] Warsaw University of Technology, Faculty of Civil Engineering, Mechanics and Petrochemistry, Poland
[b] Institute of Fundamental Technological Research, Polish Academy of Sciences, Pawińskiego 5B, 02-106 Warszawa, Poland

HIGHLIGHTS

- A procedure of specimen preparation of homogeneous RH a desired value was proposed.
- API of shielding concrete in oven dry state and at a specific, stabilized RH was determined.
- Linear relationship between API and concrete RH in range of 2% to 99% was found.
- The influence of the type of aggregate for shielding concrete on API value was determined.

ARTICLE INFO

Article history:
Received 5 February 2017
Received in revised form 22 April 2017
Accepted 23 April 2017

Keywords:
Autoclam air permeability
Relative humidity
Heavyweight aggregate
Barite
Magnetite
Serpentine
Radiation shielding concrete
Slag cement

ABSTRACT

The permeation properties of concrete are strongly influenced by the degree of saturation of capillary pores. Test results of the Autoclam air permeability index (API) of radiation shielding concrete are presented. Concrete specimens were made with CEM I and CEM III/A cements and special aggregates for radiation shielding: crushed barite, magnetite, serpentine and amphibolite. Two procedures of accelerated drying with simultaneous measurement of moisture distribution in the specimens were proposed. The specimens were tested at different RH levels from a fully saturated state to an oven dried state. The linear relationship between the API and RH was obtained. Effects of heavyweight and hydrogen-bearing aggregates on air permeability index were revealed.

1. Introduction

The essential criteria for concrete mix design for shielding structures of nuclear power plants include both shielding against ionizing radiation, mechanical and physical properties and also durability under severe environmental conditions [1,2]. Criteria for the selection of concrete components are related to plant operation conditions, especially neutron and gamma radiation, and also elevated temperature, which is cyclically variable in relation to the reactor fuel cycles. Moreover, concrete in load-bearing shielding structures should meet the requirements of strength, elasticity and impermeability to liquids and gases – also in emergency conditions [3–5]. The impermeability of concrete with regards to potentially contaminated air and water (due to e.g. the leaking of a reactor's cooling system) is one of the basic indicators of the functional suitability of a biological shield [6]. Low permeability also prevents against the penetration of harmful substances into concrete, which could lead to the corrosion of steel reinforcement or the destruction of concrete, as in e.g. spent fuel pools. The assessment of the permeability of concrete should take place in environmental conditions that are representative of the place of its usage.

Shielding concrete is prepared using special components, which are selected due to their neutron and gamma radiation shielding properties. Heavy aggregates such as barite, magnetite and hematite, which contain elements with a high atomic number, provide effective shielding for the γ radiation. For protection against neutron radiation, aggregates that contain elements with a low atomic number, a large amount of bound water and also boron in

* Corresponding author.
E-mail address: wojciech.kubissa@pw.edu.pl (W. Kubissa).

http://dx.doi.org/10.1016/j.conbuildmat.2017.04.177
0950-0618/

their composition are the most effective [7,8]. Special aggregates, ASTM C637 [9], generally made of soft rocks, are sometimes characterized by unfavourable gradation and a high content of dust that cause an increase of water demand and technological difficulties in the manufacturing and compaction of concrete mix [6]. As a result, it is difficult to keep low water/cement ratio of the mix while maintaining the desired homogeneity and consistency of concrete mix. Therefore an increased permeability of concrete made of the above-listed special aggregates can be expected.

The measurement of concrete permeability can be carried out using various methods. It is important that the measuring method enables concrete to be assessed at the stage of the design of its composition and also during a periodic inspection of concrete permeability in structural elements. The recommendations of IAEA [1] regarding nuclear containments suggest three methods of determining the air permeability of concrete, i.e. the Torrent method [10], the Autoclam method [11] and the method of surface airflow [12]. Comparative analysis of various methods that was presented in [13] indicated that the criteria for the evaluation of permeability (categories of concrete permeability) are generally defined with respect to specimens dried at a temperature of 105°C up to a constant mass. This applies to the methods of Torrent and Autoclam, as well as to the method of RILEM – Cembureau. There were also attempts to dry the surface of a concrete specimens using different methods [14], however they did not give satisfactory results. Numerous studies have shown that air permeability depends largely on the water content in concrete [15–17]. Therefore, correction coefficients and diagrams are used to approximately determine the surface moisture content of concrete on the basis of an electrical resistance measurement [18]. Due to the occurrence of near-surface moisture gradients [19] such dependence is difficult to establish.

The determination of the air permeability of concrete in a state of partial saturation of water meets the requirements of operation in nuclear power shielding constructions. On the basis of measurements of temperature and the relative humidity of concrete, Oxfall et al. proved the variability of hygrothermal parameters in different parts of single-shelled containment walls of a nuclear reactor [20]. Representative environmental conditions are determined by the temperature of concrete ranging from 50 to 65°C, and also a relative humidity (RH) from 40 to 60%. With the exception of the concrete layer in the close vicinity of a reactor, the relative humidity of concrete is maintained at this level after many years of reactor operation. The water content in concrete is also important with regards to shielding against neutron radiation [21], as hydrogen contained in water contributes significantly to neutron thermalization. Therefore, characterization of concrete as a shielding material, both against ionizing radiation and also against the infiltration of potentially contaminated air, should take into account water saturation.

The study of [22] focused on the tightness of the containment walls of nuclear power plants in the case of an accident caused by a loss of coolant, resulting in increased air–steam mixture pressure at an increased temperature to about 140°C. The effects of induced stresses and microcracks on the tightness integrity of a concrete wall were particularly studied. The results indicated that the degree of saturation level significantly affected the gas mixture leakage rate through undamaged concrete specimens. The vaporization of free water and the thermal expansion of water could create strong moisture gradients that are able to cause micro-cracks and influence permeability. It was suggested that the greater the initial water content, the more concrete porosity increases, and thus the water vapor leakage rate will therefore be greater. The authors of [23] proposed to spray water on dry and cracked concrete as a method to recover a large part of its gas tightness.

A low permeability of concrete is considered to prevent any significant leakage in undamaged zones but the air flow rate in containment buildings is significantly influenced by cracks [24,25]. The effects of microcracking on the air permeability of concrete, considered very relevant to the containment integrity evaluation, were studied for structural concrete by Wu et al. [26]. It was found that microcracking increased when the drying regime became more severe. The authors concluded that drying-induced microcracks must be considered when interpreting and comparing permeability results. However, the issue of permeability of damaged concrete is not pursued in this study.

The determination of concrete air permeability in a specified state of water saturation was considered in the works [27–30]. The authors highlighted the fact that specimens should be brought to the same humidity before testing due to the significant impact of concrete humidity on the results of permeability tests. However, frequently used intensive drying at a temperature of 105°C results in concrete damage, the formation of microcracks and also chemical changes, which affect the permeability test results. Proposals of specimen preparation methods that do not require drying at a temperature above 50°C have therefore been presented. The authors draw attention to the need to test specimens with a uniform specified humidity and to also determine the dependency between permeability and concrete humidity.

A significant impact of concrete composition on gas permeability is primarily known with regards to w/c ratio and also the content and type of supplementary cementitious materials. An improvement in the impermeability of concrete containing fly ash is assigned to pozzolanic reaction effects and also changes in the phase composition of hardened cement paste [28,31,32]. It has been found that the use of multi-component cements that contain fly ash and also granulated blast-furnace slag or limestone causes a reduction in air permeability [33]. The results of tests [19] proved that an increase in w/c ratio from 0.45 to 0.55 resulted in more than a twofold increase in air permeability. The influence of w/c ratio is crucial – according to [34] it is the basis when considering the usefulness of air permeability measurements in the assessment of the suitability of concrete in XC exposure classes according to PN-EN 206 [35].

The influence of type of aggregate on the air permeability of concrete was not systematically studied for radiation shielding concrete, however some results regarding aggregates used in ordinary concrete are known [36–38]. A significant decrease in air permeability was noticed when replacing granite aggregate for crushed marble aggregate. Microscopic analysis of the contact zone between grains and cement paste showed more detachments in the case of granite aggregate. It has been suggested that the type of aggregate mineral has an influence on the formation of defects and cracks in the contact zone, and this zone's defects contribute to an increase of airflow in the capillary pore system of the cement paste. It has been noticed, regardless of the type of aggregate, that there is a decrease in air permeability with a reduction of the aggregate grain size or a decrease of coarse aggregate content in the mix. It seems to be related to a better packing density aggregate grains.

The objective of the research undertaken by the authors is to determine the impact of special aggregates on the air permeability of shielding concrete at its specified humidity. In order to control the humidity of concrete, two variants of the methodology of preparing and testing concrete specimens have been developed. The scope of research does not include effects of the w/c ratio or the content of supplementary cementitious materials in concrete, but it does include the effects of using CEM I and CEM III/A cements i.e. Portland cement and slag cement.

2. Description of experimental tests

2.1. Materials and specimens

Tests were carried out on specimens of shielding concrete designed with various types of mineral aggregates with regards to shielding against gamma and neutron radiation. Following the principles of shielding concrete design [7,21,39], the following types of aggregates were selected:

- magnetite aggregate with 0–16 mm and 0–5 mm fractions (a density of 4800 kg/m^3),
- barite aggregate with 0–16 mm fraction (a density of 4200 kg/m^3),
- serpentine aggregate with 0–2 mm, 2–8 mm and 8–16 mm fractions (a density of 2600 kg/m^3),
- amphibolite aggregate with 2–8 mm and 8–16 mm fractions (a density of 2900 kg/m^3).

Quartz sand with a density of 2650 kg/m^3 was also used.

The following two types of cement of low heat of hydration, high resistance to sulphate and reduced alkali content were used: CEM I 42.5 N LH/SR3/NA and CEM III/A 42.5 N LH/HSR/NA. The composition and physical properties of cements is presented in detail in [40]. In the design of concrete mixes an equal amount of cement and the water-cement ratio was assumed, namely: 350 kg/m^3 and w/c = 0.48 in the first series of mixes and 340 ± 4 kg/m^3 and w/c = 0.486 ± 0.005 in the second series. In order to keep a similar consistency of all the mixes that were denoted by the slump test, water reducing admixtures in variable amounts were used. The composition of concrete mixes with CEM I and CEM III/A cements is given in Tables 1 and 2, respectively [39].

Concrete mixes with CEM I cement were made in laboratory conditions in a concrete mixer with a capacity of 50 L using aggregates in a surface-dry state. The concrete mixes with CEM III/A cement were also made in a laboratory concrete mixer but the aggregates were used in a natural humidity state due to them being stored in a commercial concrete batching plant. The consistency of the concrete mixes was determined with a slump test in accordance with PN-EN 12350-2 [41]. It ranged from 40 mm to 120 mm for the series with CEM I cement and from 40 mm to 190 mm for the second series, except for mixes B12, B13 and B14 that showed only 20 mm of slump. The following specimens were manufactured:

- – 150 mm cube specimens for compressive strength determination,
- – slabs with dimensions of 230 × 230 × 100 mm for the first series and 150 mm cube specimens for the second series in order to determine air permeability.

Curing of specimens was carried out in accordance with the requirements of PN-EN 12390-2 [42] in conditions of high relative humidity >96% and a temperature of 20 ± 2°C for a period of 28 days (series I) or for at least half a year (series II).

2.2. Testing methods

A standard method in accordance to PN-EN 12390-3 [43] was used to determine the compressive strength. The concrete air permeability index (API) was measured using an Autoclam device from Amphora Company [44]. An applied modification of the procedure included the attachment of an annular seal made of microgum with a thickness of 8 mm, clamping of a steel base ring was achieved using G-clamps instead of expansion anchors in bored holes (Fig. 1). The compliance of API readings obtained in such a way was confirmed experimentally.

The dimensions of slab specimens of 230 × 230 × 100 mm were selected, as was the case in the studies [27]. The API was determined in a central point on the two opposed bigger surfaces of the specimen.

The determination of relative humidity and temperature in concrete pores was performed using HMP44 probe from Vaisala Instruments Company, as was the case with [20]. The probes were put into holes with a diameter of 16 mm in plastic tubes at a certain depth from the specimen surface:

- 50 mm below the surface of slabs that have dimensions of 230 × 230 × 100 mm (in the middle of their thickness).
- 30 mm and 75 mm below the surface of cubic specimens that have an edge equal to 150 mm.

A special cylindrical chamber with a Vaissala probe that tightly adheres to the surface was designed for measuring relative humidity at the specimen surface.

After curing the specimens were subjected to systematic drying in a temperature chamber with a forced air flow, a fixed temperature of 50°C (series I) or 65°C (series II) and air relative humidity <10%. RH readings in concrete at different depths were made just before the beginning of drying of specimens and also at various stages of drying. The measurements of API and RH were carried out at a minimum of weekly intervals after the specimens had been cooled for 24 h to the air temperature in the laboratory room, which was equal to 20°C ± 2°C. Drying at a temperature of 50°C lasted for two months.

Table 1
The composition of concrete mixes with CEM I cement [kg/m^3] (series I).

Components	Mixture ID				
	B4	B21	B22	B25	B26
CEM I 42.5NLH/SR3/NA	350	350	350	350	350
Sand 0–2 mm	593	371	371	0	371
Amphibolite 2–8 mm	628	0	0	0	0
Amphibolite 8–16 mm	750	0	0	0	0
Magnetite 0–5 mm	0	839	0	0	0
Magnetite 0–16 mm	0	1846	0	0	0
Serpentine 0–2 mm	0	0	273	0	0
Serpentine 2–8 mm	0	0	909	0	0
Serpentine 8–16 mm	0	0	273	0	0
Barite 0–16 mm	0	0.00	0	2936	2349
Optima 100	1.40	2.35	6.90	2.59	0.88
Optima 185	0	0	3.96	0	0
Water	168	168	168	168	168
Bulk density [kg/m^3]	**2492**	**3524**	**2324**	**3412**	**3206**

Table 2
The composition of concrete mixes with CEM III/A cement [kg/m^3] (series II).

Components	Mixture ID							
	B11	B12	B13	B14	B15	B16	B17	B18
CEM III/A 42.5N-HSR/NA	341	341	342	344	337	342	336	345
Sand 0–2 mm	361	361	362	365	0	363	356	365
Serpentine 0–2 mm	0	266	0	0	0	0	0	0
Serpentine 2–8 mm	0	885	473	477	0	0	466	776
Serpentine 8–16 mm	0	266	0	477	0	0	0	179
Magnetite 0–5,6 mm	816	0	753	879	0	0	0	0
Magnetite 0–16 mm	1796	0	994	0	0	0	0	0
Barite 0–16 mm	0	0	0	0	2828	2298	1504	771
Optima 100	0.99	1.92	1.45	0	0.98	0.61	1.76	1.94
Optima 185	1.02	5.11	0	1.46	0	0	0	3.1
Water	163	163	164	165	162	164	161	165
Bulk density [kg/m^3]	**3479**	**2289**	**3089**	**2708**	**3328**	**3168**	**2825**	**2606**

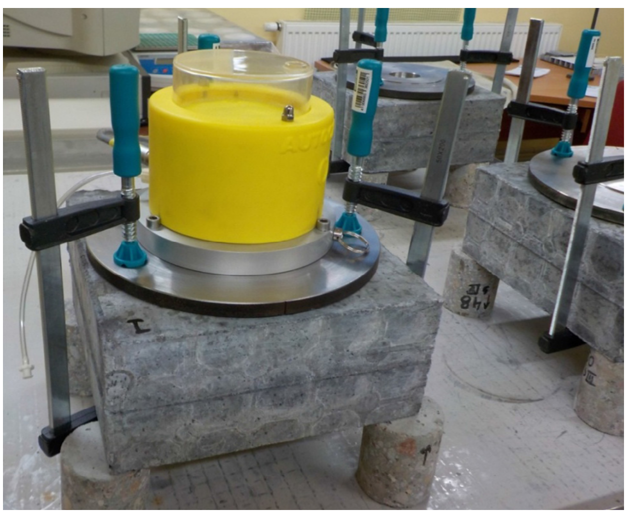

Fig. 1. View of the clamping of base ring on a specimen during testing of air permeability index using an Autoclam device.

Drying at a temperature of 65°C lasted until the moment of achieving a RH below 65% in concrete at a depth of 30 mm from the surface. The specimens were then tightly wrapped in aluminium foil and stretch film and left in a laboratory room at a temperature of 20°C ± 2°C to stabilize the humidity in the specimens (i.e. to uniform the moisture distribution). The mass of each specimen was also measured while measuring API and RH. Finally, the specimens were oven dried to a constant mass at a temperature of 105°C and then, after being cooled to a temperature of 20°C ± 2°C, measurements of the mass of specimens and API and RH in concrete were taken. Four adjacent walls of the cubic specimens had a resin insulating layer, which is impermeable to air, applied on them. The API was determined in a central point on two opposite non-isolated side surfaces. Clamping of a steel base ring was in this case achieved also using G-clamps, placed in four corners of the specimen (Fig. 2).

3. Test results

The relationship between the air permeability index and the relative humidity of concrete for the series of specimens with CEM I cement is shown in Fig. 3. An increase of the API from about 0.10 to 0.47 ln(mbar)/min, with the reduction of the RH from a state of full saturation to a dried state, was observed. The difference of the slope coefficient was influenced by the aggregate type and content and ranged from 0.208 to 0.326, whereas the extreme values were found for concrete with magnetite aggregate (B21) and for concrete with barite aggregate (B26).

Table 3 shows the time of drying of concrete specimens, the time of stabilizing the humidity distribution and also the values of RH measured on both the specimen surfaces and at a depth of

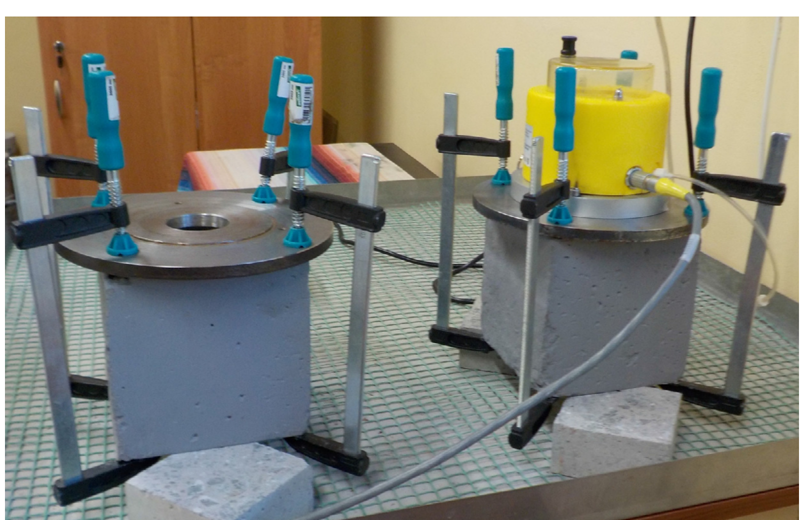

Fig. 2. View of the clamping of base ring on a cubic 150 mm specimen.

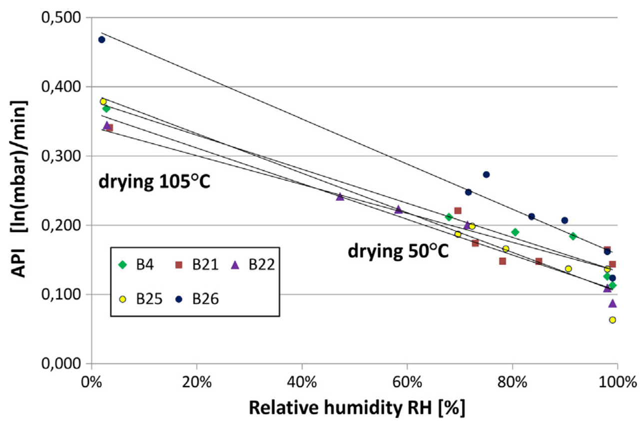

Fig. 3. The relationship between the air permeability index and RH of concrete.

30 mm and 75 mm. At the beginning of drying the RH in concrete at a depth of 30 mm ranged from 83% to 92%. The drying time required for achieving the targeted RH = 65% at a depth of 30 mm ranged from 37 days in the case of serpentine concrete (B12) to 57–58 days in the case of concrete comprising primarily of magnetite with a grain size of 0–16 mm (B11 and B13). The total drying and stabilization time ranged from 128 days for B18 concrete to 141 days for B13 concrete.

An important observation resulting from the distribution of the RH shown in Table 3 is a considerable variation in the surface humidity when RH at a depth of 30 mm decreases below 65%. Concrete specimens that contained serpentine aggregate required a shorter drying time and this resulted in the achievement of higher values of the RH on the concrete surface at the end of the drying process, i.e. 38.1%, 41.8% and 30.5% for concrete series B12, B14 and B18 respectively. Concrete specimens that contained a large amount of magnetite with a grain size of 0–16 mm required the longest drying time and obtained low RH surface values equal to 22.0% and 23.6%.

The measurements of RH inside specimens indicate a different distribution of the relative humidity along the specimen thickness immediately after finishing drying and after a period of RH stabilization. The applied procedure of stabilizing the RH proved to be effective. A significant decrease in the differences of RH on the surface and in the middle of a specimen was found – the distribution of RH along the thickness was close to constant distribution. In the stabilization period there was a diffusion of moisture from the inside of a specimen towards its surface area and this caused RH inside to decrease by 2–7%, whereas RH at the surface increased by up to even 30%. Non-uniform distribution of RH without stabilization means that the results obtained are less accurate than the ones obtained after the stabilization period.

An exemplary diagram of changes of the RH and the mass of specimens during drying and stabilization is shown in Fig. 4. RH in concrete at a depth of 75 mm (in red) and 30 mm (in blue) is marked with continuous and dotted lines. The continuous line represents the period of drying at a temperature of 65°C, whereas the dotted line indicates the period of RH stabilization at a temperature of 20°C. The horizontal dotted lines denote the RH values on the surface of specimen after the period of drying at a temperature of 65°C (a lower value) and also after RH stabilization.

The specimen mass only varied during drying. During the RH stabilization period the mass change was smaller than 0.05% of a specimen mass. After the stabilization period B12 specimens showed the smallest difference between the RH on the surface and at a depth of 75 mm. The B15 specimens showed the biggest difference of RH when comparing the RH measured on the surface with that inside the specimen. Such differences amounted to 5.0% and 18.6% respectively.

Table 4 shows the decrease in RH, which was measured at a depth of 30 mm and 75 mm during drying at a temperature of 65°C and also during RH stabilization period. The loss of water was similar for all the specimens. The maximum value, equal to 184.0 g in the B14 concrete, was about 12.5% greater than the minimal value that was equal to 163.5 g for the B16 concrete. The percentage differences are greater, however, this mainly results from the intentional variable density of concrete mixes with different types of aggregates.

The substantial decrease in the RH when drying at a temperature of 65°C at a depth of 30 mm and 75 mm ranged from 28.0% in the B16 concrete to 16.8% in the B15 concrete. The initial value of the RH, which ranged from 82.9% at a depth of 30 mm in the B12 specimens to 94.2% at a depth of 75 mm in the B13 specimens, had a big impact on the differences of the RH during the drying process. The decrease of the RH from a value of over 90% to 78–80% was fast; usually one week of drying was followed by a decrease of even 10%. Subsequent drying was much slower.

During the stabilization process the decrease in RH at a depth of 30 mm ranged from 2.1% in B12 concrete to 3.8% in B18 concrete. The difference is not significant considering the fact that the accuracy of a measuring device is equal to 2.0% in such a measurement range of RH. Larger differences of RH during the stabilization of humidity were observed at a depth of 75 mm. The biggest differences were observed in B12 and B18 specimens, which mainly contained serpentine aggregates, and they amounted to 7.4% and 7.1%. The smallest differences, equal to 2.9% and 3.2%, were noticed in B11 and B13 specimens, which mainly contained magnetite aggregates. The specimens with serpentine needed a shorter drying time to achieve the required RH below 65% at a depth of 30 mm, and the most uniform distribution of humidity was obtained after a period of stabilization.

Fig. 5 shows the average API and standard deviations of six measurements obtained after the stabilization of humidity in specimens and after drying the specimens at a temperature of 105°C. A small scatter of results was seen after RH stabilization. The coefficients of variation ranged from 13.1% for B11 specimens to 20.7% for B12 specimens.

Table 3
The relative air humidity in the pores of concrete at a specified depth and RH at the specimens surface.

Concrete ID	Drying time	RH after drying at 65°C [%]			Stabilization time	RH after stabilization [%]		
	[days]	Surface	30 mm	75 mm	[days]	Surface	30 mm	75 mm
B11	57	22.0	64.7	72.8	83	52.1	61.4	70.0
B12	37	38.1	63.7	72.4	98	58.3	60.8	63.3
B13	58	23.6	63.3	71.7	83	50.6	59.3	66.6
B14	41	41.8	63.5	71.2	96	57.6	61.6	65.7
B15	51	21.1	64.9	74.4	89	53.0	62.4	71.6
B16	43	24.7	63.5	73.3	91	52.6	59.8	68.4
B17	42	26.1	64.6	74.2	91	55.8	62.2	69.0
B18	40	30.5	64.5	70.7	88	53.6	60.1	62.9

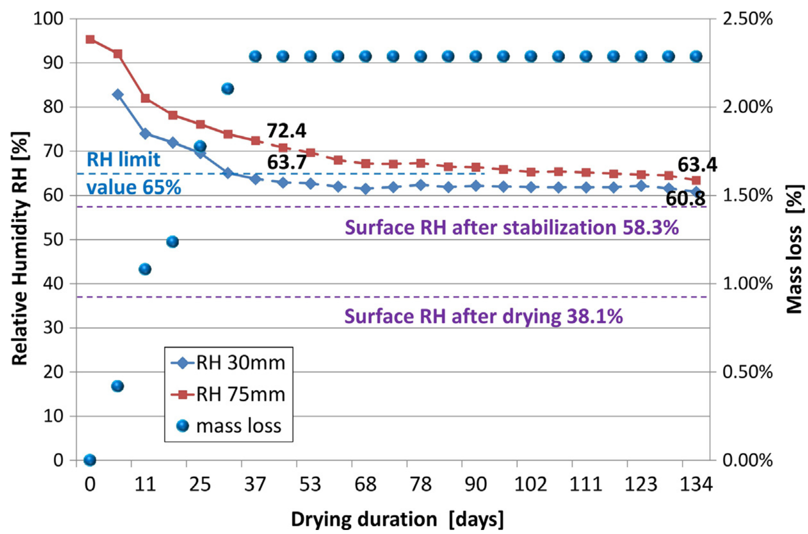

Fig. 4. RH in B12 concrete during drying (continuous) and humidity stabilization (dotted). (For interpretation of the references to colour in this figure legend, the reader is referred to the web version of this article.)

Table 4
The decrease of the RH and specimen mass during drying and RH stabilization process.

Concrete ID	RH decrease [%]				Decrease of specimen mass	
	Drying		Stabilization		During drying	
	Depth of 30 mm	Depth of 75 mm	Depth of 30 mm	Depth of 75 mm	[g]	[%]
B11	24.2	20.0	2.8	2.9	174.6	1.5
B12	20.0	21.3	2.1	7.4	180.1	2.3
B13	25.4	22.4	3.2	4.1	183.9	1.8
B14	22.8	24.3	2.7	5.9	184.0	2.0
B15	25.3	16.8	2.8	3.2	174.0	1.5
B16	28.0	18.7	3.7	4.9	163.5	1.5
B17	25.0	18.1	3.0	5.4	178.0	1.8
B18	23.4	21.7	3.8	7.1	180.3	2.0

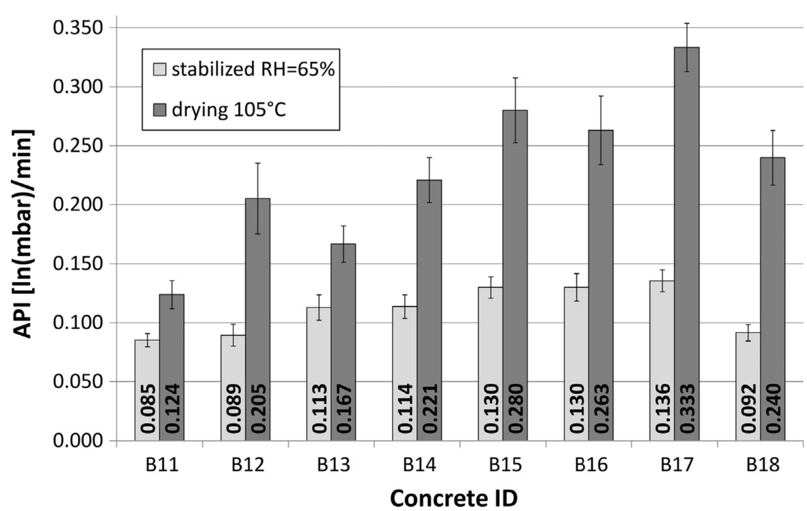

Fig. 5. Air permeability index after specimens drying and RH stabilization to 60–65% and after subsequent drying at 105 °C.

The lowest air permeability index, equal to 0.085 ln(mbar)/min, was found in the case of B11 specimens, which contained magnetite and sand. Concrete specimens that contained mainly serpentine aggregates had a slightly higher API. The difference was equal to 4.9% in the case of B12 specimens and 7.3% for B18 specimens, which both contained an addition of the barite aggregate. The test of two mean values at the significance level of $\alpha = 0.05$ did not show a significant difference between the API of these three series of specimens. Concrete specimens containing magnetite and serpentine aggregates showed a higher API than B11 specimens. It was higher by 32.4% in the case of B13 specimens and by 33.3% for B14 specimens. The highest air permeability index was

Table 5
The compressive strength of concrete of series I and the estimated value of API when RH = 60%.

Concrete ID	B4	B21	B22	B25	B26
Compressive strength f_{c28} [MPa]	56.2 ± 2.6	64.3 ± 1.9	43.9 ± 2.4	54.7 ± 4.2	50.3 ± 1.1
API when RH = 60% [ln(mbar)/min]	0.232	0.217	0.209	0.218	0.288

Table 6
The compressive strength of concrete specimens with CEM III/A cement (series II).

Compressive strength [MPa] of concrete	Concrete ID							
	B11	B12	B13	B14	B15	B16	B17	B18
at 28 days	62.0 ± 4.1	58.1 ± 5.5	66.2 ± 3.5	70.2 ± 3.7	59.9 ± 2.4	54.3 ± 6.2	61.4 ± 4.0	60.4 ± 5.7
at 90 days	80.8 ± 6.4	77.8 ± 3.9	84.6 ± 3.3	90.6 ± 9.3	61.7 ± 5.1	59.6 ± 0.9	68.5 ± 4.0	66.6 ± 1.5

observed in concrete specimens containing mainly barite aggregates, namely: B15, B16 and B17. The API differences in relation to the B11 specimens amounted to 52.3%, 52.4% and 58.8%, respectively. Applying the criteria presented in Basheer [44] one can classify B11, B12 and B18 concrete as "very good". The results of the other concrete allows to classify them as "good".

In the case of the specimens dried at a temperature of 105°C, the scatter of API results was slightly bigger. The coefficients of variation ranged from 12.3% for B17 specimens to 31.6% for B18 specimens. The lowest air permeability index, equal to 0.124 ln (mbar)/min, was found for B11 specimens, which contained magnetite and sand. The aggregate-related dependencies of API were similar to these observed at 60–65% RH, but the relative difference between the results increased. The difference between maximum and minimum API values increased by approximately threefold comparing to 60–65% RH results.

Table 5 shows the compressive strength of the concrete after 28 days of curing. The API values that were estimated using an approximate linear relationship when the RH = 60% were also presented. Due to the fact that the compressive strength is in a range between 43.9 MPa and 64.3 MPa and the estimated air permeability index changes within ±20%, no clear correlation between these parameters can be stated.

The results of the determination of the strength of series II concrete, which are presented in Table 6, indicate that the 28-day compressive strength of the concrete specimens was in a range of 60 MPa to 70 MPa. In the case of the concrete with magnetite and serpentine aggregates, a significant increase in strength ranging from 27.9% for the B13 concrete to 33.8% for the B12 concrete obtained from 28 to 90 days of maturation was observed. The increase in strength between 28 and 90 days of maturation was significantly lower in the case of the concrete containing barite aggregates and ranged from 3.0% for the B15 concrete to 11.7% for the B17 concrete. There was no clear correlation between the API and the compressive strength of series II concrete.

4. Discussion

The criteria for assessing the quality of concrete on the basis of API are known from Basheer [44] and they are related to concrete dried at a temperature of 105°C. Results of API determination in the containment walls of a reactor at a nuclear power plant in southern China, built in 1997, were assessed on this basis [45]. Tests involved two containment structures made of prestressed concrete. API indices were obtained in a range from 0.05 to 0.17 ln(mbar)/min in the first structure, and from 0.04 to 0.15 ln (mbar)/min in the second structure. This classified them into groups of concrete with a good and very good quality. However, neither the moisture state of concrete in the containment nor a significance of possible carbonation in cover concrete were known. These factors could affect the positive assessment of the quality of concrete.

A significant influence of the type of a heavy aggregate on API was found. When comparing the results on concrete specimens with a RH = 55–65%, the lowest API was found in concrete containing magnetite. The specimens containing mainly serpentine aggregate had a slightly higher API. The highest air permeability index was observed in concrete specimens containing mainly barite aggregate. API values of concrete with magnetite aggregate were even lower in comparison to concrete with amphibolite aggregate of a favourable grain size distribution, which was assumed as a good quality reference concrete. Such observation was similar to studies [36,37] and probably stems from a better packing of aggregates.

Systematic tests of API on radiation shielding concrete were not reported, however a comparison with API data on common structural concrete can be made. The obtained air permeability index of the concrete with magnetite aggregate was about 40% higher than API of the high-performance concrete with a varied composition, a water/binder ratio equal to 0.30, which was tested at a similar RH resulting from several weeks of drying at a temperature of 50°C [27,30]. Investigation of Basheer et al. [19] was related to concrete with w/c ratio of 0.45 and 0.55 that was made with basalt aggregate of up to 10 mm and natural sand. When having a similar average RH of concrete with w/c ratio equal to 0.45, the obtained API was comparable to the API determined for shielding concrete from series II.

In recent articles regarding the permeability test with the use of an Autoclam device [27,32,46], there are recommendations to avoid correction coefficients when calculating the air permeability index if RH in the surface layer of concrete is lower than 65%. It is assumed that with such RH most of the moisture is removed from its capillaries and it has no significant influence on the permeability measurement. Authors of studies [15,16], when testing permeability using the method of Torrent or Cembureau, show the linear dependences between the permeability coefficient K or kT expressed in logarithmic scale and the degree of concrete saturation expressed in linear scale. Presented relationships are similar to the influence of RH on API for RH in the range from 55 to 90% [46] measured at a depth of 20 mm and for RH range from 45 to 75% [27] measured at a depth of 40 mm from the specimen surface.

Concrete specimen drying to a constant mass at a temperature of 105°C results in considerable damage to concrete [25,27,30]. Such heating induces cracks that are mainly the result of differences in the thermal expansion of the individual components of concrete. There could be also changes in microstructure, e.g. the beginning of ettringite decomposition or the release of physically bound water. Table 7 shows an increase of the air permeability

Table 7
The relative increase in the API due to concrete drying at a temperature of 105 °C to RH less than 10% in comparison to specimens at RH of about 60%.

Concrete ID	B11	B12	B13	B14	B15	B16	B17	B18
Increase of API	45%	127%	48%	134%	115%	110%	155%	145%

index in specimens after being dried at a temperature of 105°C to RH less than 10% compared to specimens at RH = 55–65% in concrete.

Depending on the type of aggregate, damage caused by the drying process at a temperature of 105 °C caused a significantly different increase in the API. The lowest increase occurred in the series that contained mainly magnetite. In the case of the barite aggregate, the higher increase in the API can be explained by the higher thermal expansion of this aggregate when compared with the magnetite aggregate. The thermal expansion of magnetite and the cement matrix is similar, while for barite aggregate it is about two times higher [47]. The highest increase in permeability, which was noted in the case of concrete with serpentine aggregate, is difficult to explain. For an unknown reason the reduced tortuosity of a pore system, which was caused by heating at a temperature of 105°C, was suddenly revealed.

According to [28], RH of concrete measured at a depth of 40 mm from the surface is representative for API determination. When measuring RH on the concrete surface and at depths of 10, 20, 30 and 40 mm, authors found a significant impact of the drying process on RH related only to the outer layer with a thickness of 10 mm, with no significant differences of RH at deeper depths. Results of RH distribution during drying of series II specimens confirmed these observations. When drying the specimens at a temperature of 65°C, the difference between RH measured in holes at 75 mm and at 30 mm from the surface ranged from 6.2% to 9.8% in B18 and B16 concrete specimens, respectively. The differences between RH at a depth of 30 mm and at the surface ranged from 21.7% to 43.8%, for B14 and B15 specimens, respectively. Observed humidity gradients were significantly higher at layers closer to the specimen surface.

Due to the use of different specimens (size, age) and the conditioning differences, a direct comparison of the results of series I and II is not possible. Similar qualitative influence of aggregates in radiation shielding concrete on API was observed for series I specimens (predicted at RH = 50%) and for series II specimens at measured RH after its stabilization. Concrete specimens B21 and B22 with magnetite and serpentine showed the lowest and closest to each other API values. The air permeability index for B26 concrete with barite aggregate and sand was 32.7% higher than for B21 concrete. API determined on concrete specimens that contained only barite was similar to the result of B21 concrete.

The API of series II were calculated with the assumption of a linear dependency of the API from RH, and compared with the experimental results obtained for specimens with stabilized RH. Coefficients A and B of the equation of a straight line passing through point [x1 = 0,99; y1 = 0,06] and [x2 = RH after drying at a temperature of 105°C; y2 = API after drying at a temperature of 105°C] were calculated with the assumption of the same value of the API equal to 0.06 ln(mbar)/min in the case of concretes with different compositions fully saturated with water (when RH = 99%). The value of the API_{calc} with the same RH as the one obtained after the period of stabilization was calculated based on the equation of a straight line and then compared with the achieved experimental result API_{test} The error of such a determined value ranged from −8% in the case of the B13 concrete to 38% in the case of the B18 concrete. The calculated values are given in Table 8.

The results determined on the basis of the linear dependence between the API and the RH are close to the experimental results for the concrete containing magnetite and barite. In the case of the concrete with serpentine, the error is larger and ranges from 25% to 38% for the B17 and B18 concrete.

The suitability of the specified linear relation for the determination of the API at any level of RH is limited. The obtained values have a margin error of unknown size, which probably depends on the degree of damage to the specimens drying at a temperature of 105°C. In addition, the value of the API in the concrete completely saturated with water must be empirically determined or established and this is burdened with an unknown error. The exact determination of the API value at a specified RH requires preparation of the specimens with stable humidity and then immediate testing. It is worth noting that bringing the specimens to a state of level humidity was based on the method illustrated in the work [27]. The water vapour exchanges during drying were unidirectional in order to avoid tri-dimensional water content gradients, which are more difficult to eliminate during the redistribution steps.

Since functional criteria regarding shielding concrete include many properties, especially permeability and shielding against ionizing radiation, the obtained results are presented in Figs. 6 and 7 using the concept of the multi-criteria optimization for concrete mix design [48]. In absence of experimental data, the shielding properties of concrete can be roughly estimated on the basis of the composition [7,21] considering the following assumptions:

a) shielding against gamma radiation is proportional to the density of concrete,
b) shielding against neutron radiation can be related to the content of hydrogen in concrete ingredients, i.e. the water content.

Table 8
Coefficients of the adjustment of a straight line to a dependency between the API and the RH in a range between 55% and 65% after stabilizing to below 10% due to drying at a temperature of 105 °C.

Coefficients of the equation of a straight line and compliance parameters	Concrete ID							
	B11	B12	B13	B14	B15	B16	B17	B18
$API_{RH=99\%}$	0.06	0.06	0.06	0.06	0.06	0.06	0.06	0.06
RH_{dry}	2.0%	3.9%	2.3%	3.1%	2.9%	2.6%	2.2%	2.9%
API_{dry}	0.124	0.205	0.167	0.221	0.280	0.263	0.333	0.240
A	−0.066	−0.153	−0.110	−0.168	−0.229	−0.211	−0.282	−0.187
B	0.125	0.211	0.169	0.226	0.287	0.269	0.340	0.245
RH_{stab}	61.2%	60.8%	58.8%	61.6%	62.3%	60.3%	62.3%	58.9%
API_{calc}	0.085	0.118	0.104	0.123	0.144	0.142	0.164	0.135
API_{test}	0.085	0.091	0.113	0.094	0.130	0.125	0.131	0.098
Difference	0%	31%	−8%	30%	11%	13%	25%	38%

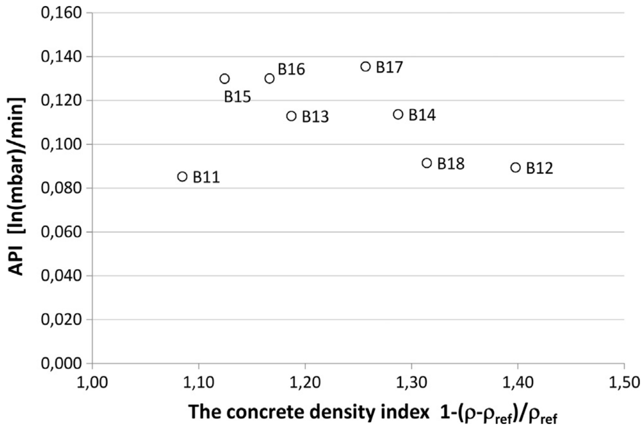

Fig. 6. Air permeability index as a function of concrete density index.

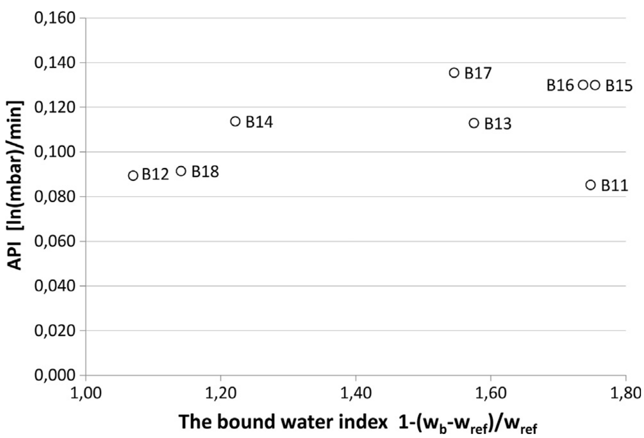

Fig. 7. Air permeability index as a function of bound water index (CEM I – theoretical bound water content, CEM II/A-experimentally determined bound water content).

To estimate the shielding properties, two appropriate dimensionless indexes were used:

a) the concrete density index: $1 - (\rho - \rho_{ref})/\rho_{ref}$, where ρ and ρ_{ref} are the density according to Tables 1 or 2 and the reference – maximum density (3800 kg/m^3 – an arbitrary assumption), respectively,
b) the bound water index: $1 - (w_b - w_{ref})/w_{ref}$, where w_b and w_{ref} are the content of bound water in concrete (in hardened cement paste and aggregate grains) and the reference water content in the mix (300 kg/m^3 – an arbitrary assumption), respectively.

The amount of bound water in the serpentine aggregate that is equal to 12.0% was determined experimentally using a method in accordance with ASTM C637 [9]. The amount of bound water in hardened cement paste depends on the phase composition of the cement, on the degree of hydration and also on the way the term "bound water" is defined [49,50]. The content of bound water in concrete with CEM III/A cement was experimentally determined using TGA analysis.

With such a selection of relative performance indices, both figures illustrate the set of compromise solutions for concrete composition of the best attainable air impermeability and the best shielding performance. The points closest to the origin of the coordinate system represent the mix design of the high radiation shielding and low permeability of concrete. Concrete mixes with CEM III/A cement and magnetite and serpentine aggregates were characterized by the best combination of high shielding and low air permeability properties while providing that the compressive strength was at least 54 MPa. However, such a simplified categorization of the performance of concrete mixes is not valid in the case of mixed radiation type – in such a case a direct shielding performance determination is needed.

5. Conclusions

Tests of the air permeability of radiation shielding concrete were carried out on specimens with a specified relative humidity in concrete pores using an Autoclam device. On the basis of the conducted measurements of the RH, the air permeability index and also the changes of specimen mass, the following conclusions can be drawn:

- Within the RH range between 55 and 65% the air permeability index for concrete containing barite aggregate was about 55% higher than for concrete containing other types of aggregates for radiation shielding. The lowest air permeability was found for concrete with magnetite aggregate, remarkably lower than for well-graded amphibolite aggregate.
- A linear relationship was found between the air permeability index and the RH measured at a depth of 40 mm below the tested concrete surface, covering the full range of RH values.
- Calculations of API on the basis of the API vs. RH linear relationship, and the values obtained for concrete dried at a temperature of 105°C had a margin of error of −8% to +38% of the API value when compared with experimental measurements.
- The proposed method of conditioning of concrete specimens allowed for a specified and evenly distributed RH along the cross section of cube specimens to be obtained in twenty weeks, including a required period of humidity stabilization not longer than 14 weeks.
- The usefulness of Autoclam API measuring method to assess the quality of concrete containing radiation shielding aggregates was confirmed. The proposed method of specimen conditioning and API measurement with a specific, evenly distributed RH allows to control the air of shielding concrete at the mix design stage.

Acknowledgement

The financial support from the National Center for Research and Development in Poland is gratefully acknowledged (Project PBSII/A2/15/2014 "Durability and efficiency of concrete shields against ionizing radiation in nuclear power structures").

References

[1] IAEA, Ageing Management of Concrete Structures in Nuclear Power Plants, International Atomic Energy Agency, Vienna, 2016.
[2] R. Meiswinkel, J. Meyer, J. Schnell, Design and Construction of Nuclear Power Plants, first ed., Ernst & Sohn GmbH & Co, KG, 2013.
[3] J.-M. Torrenti, G. Nahas, Durability and safety of concrete structures in the nuclear context, in: C.-B. Pedro (Ed.), Concrete under Severe Conditions, Taylor & Francis Group, London, 2010, pp. 3–18.
[4] P. Bamonte, P.G. Gambarova, Properties of concrete required in nuclear power plants, in: Infrastructure Systems for Nuclear Energy, T.T.C. Hsu, C.-L. Wu, J.-L. Lin (Eds.), John Wiley & Sons, Hobokon, NJ, USA, 2014, pp. 409–438.
[5] M.A. Glinicki, D. Jóźwiak-Niedźwiedzka, K. Gibas, M. Dąbrowski, Influence of blended cements with calcareous fly ash on chloride ion migration and carbonation resistance of concrete for durable structures, Materials 9 (1) (2016) 1–15, http://dx.doi.org/10.3390/ma9010018 (18).

[6] M.A. Glinicki, Długotrwała Funkcjonalność Betonu W Konstrukcjach Osłonowych Elektrowni Jądrowych (Longterm Performance of Concrete in Shielding Structures of Nuclear Power Plants), IPPT PAN, Warszawa, 2015.
[7] M.F. Kaplan, Concrete Radiation Shielding: Nuclear Physics, Concrete Properties, Design and Construction, Longman Scientific & Technical, Harlow, 1989.
[8] A. Brandt, Application of concrete as a material for anti-radiation shielding – a review, Cem. Wapno Beton 18/80 (2) (2013) 115–132.
[9] ASTM C637, Standard Specification for Aggregates for Radiation-Shielding Concrete, ASTM International, West Conshohocken, PA, 2014.
[10] R. Torrent, G. Frenzer, A method for the rapid determination of the coefficient of permeability of the "covercrete", in: W.G. Schickert, H. Wiggenhauser (Eds.), International Symposium Non-DestructiveTesting in Civil Engineering (NDT-CE), DGZfP, Berlin, 1995, pp. 985–992.
[11] P.A. Basheer, F.R. Montgomery, A. Long, Clam' tests for measuring in-situ permeation properties of concrete, Nondestr. Test. Eval. 12 (1) (1995) 53–73, http://dx.doi.org/10.1080/10589759508952835.
[12] D. Whiting, P.D. Cady, Condition Evaluation of Concrete Bridges Relative to Reinforcement Corrosion Volume 7: Method for Field Measurement of Concrete Permeability, Strategic Highway Research Program, Washington, DC, 1992.
[13] RILEM, Tests for gas permeability of concrete, TC 116-PCD: permeability of concrete as criterion of its durability, Mater. Struct. 32 (1999) 174–179.
[14] P. Basheer, E. Nolan, W. McCarter, A. Long, Effectiveness of in situ moisture preconditioning methods for concrete, J. Mater. Civ. Eng. 12 (2) (2000) 131–138, http://dx.doi.org/10.1061/(ASCE)0899-1561(2000) 12:2(131).
[15] L. Parrott, Moisture conditioning and transport properties of concrete test specimens, Mater. Struct. 8 (1994) 460–468, http://dx.doi.org/10.1007/BF02473450.
[16] A. Abbas, M. Carcasses, J.-P. Ollivier, Gas permeability of concrete in relation its degree of saturation, Mater. Struct. 32 (2) (1999) 3–8, http://dx.doi.org/10.1007/BF02480405.
[17] J. Liu, F. Agostini, F. Skoczylas, From relative gas permeability to in situ saturation measurements, Constr. Build. Mater. 40 (2013) 882–890, http://dx.doi.org/10.1016/j.conbuildmat.2012.11.092.
[18] M. Romer, Effect of moisture and concrete composition on the Torrent permeability measurements, Mater. Struct. 38 (2005) 541–547, http://dx.doi.org/10.1007/BF02479545.
[19] P. Basheer, E. Nolan, Near-surface moisture gradients and in situ permeation tests, Constr. Build. Mater. 15 (2–3) (2001) 105–114, http://dx.doi.org/10.1016/S0950-0618(00)00059-3.
[20] M. Oxfall, P. Johansson, M. Hassanzadeh, Long-term hygrothermal performance of nuclear reactor concrete containments – laboratory evaluations of measurement setup, in situ sampling, and moisture flux calculations, Cem. Concr. Compos. 65 (2016) 128–138, http://dx.doi.org/10.1016/j.cemconcomp.2015.10.012.
[21] ANSI, ANS-6.4, Nuclear Analysis and Design of Concrete Radiation Shielding for Nuclear Power Plants, American National Standards Institute, La Grange Park, IL, 2006.
[22] S. Medjigbodo, M. Choinska, J.P. Regoin, A. Loukili, A. Khelidj, Experimental study of the air–steam mixture leakage rate through damaged and partially saturated concrete, Mater. Struct. 49 (2016) 843–855, http://dx.doi.org/10.1617/s11527-015-0542-5.
[23] F. Agostini, F. Skoczylas, B. Masson, Sealing of concrete confining structures of French nuclear reactors, in: A.M. Brandt, J. Olek, M.A. Glinicki, C.K.Y. Leung, J. Lis (Eds.), Brittle Matrix Composites 11, Institute of Fundamental Technological Research, Warsaw, 2015, pp. 343–352.
[24] L. Jason, B. Masson, Comparison between continuous and localized methods to evaluate the flow rate through containment concrete structures, Nucl. Eng. Des. 277 (2014) 146–153, http://dx.doi.org/10.1016/j.nucengdes.2014.06.010.
[25] H. Simon, G. Nahas, N. Coulon, Air–steam leakage through cracks in concrete walls, Nucl. Eng. Des. 237 (2007) 1786–1794, http://dx.doi.org/10.1016/j.nucengdes.2007.03.025.
[26] Z. Wu, H. Wong, N. Buenfeld, Influence of drying-induced microcracking and related size effects on mass transport properties of concrete, Cem. Concr. Res. 68 (2015) 35–48, http://dx.doi.org/10.1016/j.cemconres.2014.10.018.
[27] C. Anton, M.A. Climent, G. de Vera, I. Sanchez, C. Andrade, An improved procedure for obtaining and maintaining well characterized partial water saturation states on concrete samples to be used for mass transport tests, Mater. Struct. 46 (2013) 1389–1400, http://dx.doi.org/10.1617/s11527-012-9981-4.
[28] K. Yang, P. Basheer, B. Magee, Y. Bai, Investigation of moisture condition and Autoclam sensitivity on air permeability measurements for both normal concrete and high performance concrete, Constr. Build. Mater. 48 (2013) 306–314, http://dx.doi.org/10.1016/j.conbuildmat.2013.06.087.
[29] Z. Kameche, F. Ghomari, M. Choinska, A. Khelidj, Assessment of liquid water and gas permeabilities of partially saturated ordinary concrete, Constr. Build. Mater. 65 (2014) 551–565, http://dx.doi.org/10.1016/j.conbuildmat.2014.04.137.
[30] D.R. Gardner, R.J. Lark, B. Barr, The effect of conditioning to a predetermined weight loss on the permeability of concrete, Constr. Build. Mater. 21 (2007) 83–89.
[31] K. Gibas, M.A. Glinicki, G. Nowowiejski, Evaluation of impermeability of concrete containing calcareous fly ash in respect to environmental media, Roads Bridges Drogi i Mosty 12 (2013) 159–171, http://dx.doi.org/10.7409/rabdim.013.012.
[32] K. Yang, P. Basheer, Y. Bai, B. Magee, A. Long, Development of a new in situ test method to measure the air permeability of high performance concretes, NDT E Int. 64 (2014) 30–40, http://dx.doi.org/10.1016/j.ndteint.2014.02.005.
[33] M.A. Glinicki, G. Nowowiejski, G, Strength and permeability of concrete with CEM II and "CEM V" cements containing high calcium fly ash, in: 3rd International Conference on Sustainable Construction Materials & Technologies, Professor Jan Olek Sessions on Durability and Sustainability of Concrete, Kioto, 2013, pp. 43–50.
[34] R. Torrent, E. Denarié, F. Jacobs, A. Leemann, T. Teruzzi, Specification and site control of the permeability of the cover concrete: the Swiss approach, Mater. Corros. 63 (12) (2012) 1127–1133, http://dx.doi.org/10.1002/maco.201206710.
[35] PN-EN 206, Concrete – Specification, Performance, Production and Conformity, Polish Committee for Standardization, Warsaw, 2014.
[36] D. Perraton, P.C. Aitcin, Permeability of cover concrete. Can we imagine an aggregate selection to be more determinant than the w/c ratio?, Bulletin des Laboratories des Ponts et Chausses 232 (2001) 61–74
[37] C. Argiz, M.A. Sanjuán, R. Muñoz-Martialay, Effect of the aggregate grading on the concrete air permeability, Mater. Constr. 64 (2014) 1–6, http://dx.doi.org/10.3989/mc.2014.07213.
[38] C.G. Pereira, J. Castro-Gomes, L. Pereira de Oliveira, Influence of natural coarse aggregate size, mineralogy and water content on the permeability of structural concrete, Constr. Build. Mater. 23 (2009) 602–608, http://dx.doi.org/10.1016/j.conbuildmat.2008.04.009.
[39] M. Dąbrowski, M.A. Glinicki, G. Nowowiejski, Application of special aggregates in design of radiation shielding concrete of enhanced durability, unpublished report, IPPT PAN, Warszawa, 2017.
[40] T. Baran, M.A. Glinicki, D. Jóźwiak-Niedźwiedzka, Properties of special cements for shielding concrete in nuclear power plants, Cem. Wapno Beton 21 (83) (2016) 207–215.
[41] PN-EN 12350–2, Testing Fresh Concrete. Slump-test, Polish Committee for Standardization, Warsaw, 2011.
[42] PN-EN 12390-2. Making and curing specimens for strength tests, Testing Hardened Concrete, Polish Committee for Standardization, Warsaw, 2011.
[43] PN-EN 12390-3, Testing Hardened Concrete. Compressive strength of test specimens, Polish Committee for Standardization, Warsaw, 2011.
[44] P.M. Basheer, Permeation analysis, in: V. Ramachandran, J. Beaudoin (Eds.), Handbook of Analytical Techniques in Concrete Science and Technology Principles, Techniques, and Applications, Elsevier, 2000, pp. 658–737.
[45] Y. Zheng, H.J. Li, Evaluation of protective quality of prestressed concrete containment buildings of nuclear power plants, J. Cent. South Univ. Technol. 18 (2011) 238–243, http://dx.doi.org/10.1007/s11771-011-0685-7.
[46] K. Yang, C. Yang, B. Magee, S. Nanukuttan, J. Ye, Establishment of a preconditioning regime for air permeability and sorptivity of alkali-activated slag concrete, Cem. Concr. Compos. 73 (2016) 19–28, http://dx.doi.org/10.1016/j.cemconcomp.2016.06.019.
[47] A.M. Neville, Properties of Concrete, Pearson Education Limited, Essex, 2011.
[48] A.M. Brandt (Ed.), Optimization Methods for Material Design of Cement-Based Composites, E&FN SPON, London, 1998.
[49] I. Odler, Hydration, setting and hardening of Portland cement, in: P.C. Hewlett (Ed.), Lea's Chemistry of Cement and Concrete, Elsevier, 1998, pp. 241–297, http://dx.doi.org/10.1016/B978-075066256-7/50018-7.
[50] L. Lam, Y.L. Wong, C.S. Poon, Degree of hydration and gel/space ratio of high-volume fly ash/cement systems, Cem. Concr. Res. 30 (2000) 747–756, http://dx.doi.org/10.1016/S0008-8846(00)00213-1.